BAREKENG: Journal of Mathematics and Its Applications
June 2026 Volume 20 Issue 2 Page 1513–1526
P-ISSN: 1978-7227 E-ISSN: 2615-3017
https://doi.org/10.30598/barekengvol20iss2pp1513-1526

RESIDUAL-BASED MEWMA CONTROL CHART FOR DRINKING WATER QUALITY MONITORING AT PDAM TIRTA

Agung Muhammad Takdir[1], **Erna Tri Herdiani**[2*], **Nurtiti Sunusi**[3]

[1,2,3]*Department of Statistic, Faculty Mathematics and Natural Sciences, Universitas Hasanuddin*
Jln. Perintis Kemerdekaan km10, Makassar, 90245, Indonesia

*Corresponding author's e-mail: *herdiani.erna@unhas.ac.id*

Article Info

Article History:
Received: 16th June 2025
Revised: 18th July 2025
Accepted: 6th October 2025
Available online:26th January 2026

Keywords:
Control Chart;
False Alarm;
MEWMA;
VAR-Based MEWMA;
Water Quality.

ABSTRACT

Ensuring the consistent quality of drinking water remains a major challenge in Indonesia, particularly due to natural variability and operational limitations in regional water companies (PDAMs). Statistical quality control methods such as the Multivariate Exponentially Weighted Moving Average (MEWMA) chart, are widely applied for monitoring; however, their assumption of independent and identically distributed observations reduces their effectiveness when applied to autocorrelated time-series data. This study proposes a Vector Autoregressive (VAR)-based MEWMA control chart for monitoring water quality parameters, turbidity, and residual chlorine at PDAM Tirta. Daily observations from 2023 (n = 365) were analyzed. The VAR(3) model was selected using the Akaike Information Criterion (AIC), and residuals were validated to be free from autocorrelation. These residuals were then incorporated into the MEWMA framework with a smoothing parameter $\lambda = 0.03$. A comparative analysis was conducted between the standard MEWMA and the VAR-based MEWMA through Monte Carlo simulations (5,000 replications) across three shift scenarios. Results showed that both methods achieved comparable ARL_0 values (≈3), confirming stability under in-control conditions. However, the VAR-based MEWMA consistently demonstrated lower ARL_1 values in detecting small shifts, especially in turbidity, with improvements of up to 22% compared to the standard MEWMA. These findings highlight the VAR-based MEWMA as a more sensitive and reliable monitoring tool, offering water utilities an early-warning system that enables timely corrective actions and ensures compliance with drinking water quality standards.

How to cite this article:

A. M. Takdir, E. T. Herdiani, N. Sunusi., "RESIDUAL-BASED MEWMA CONTROL CHART FOR DRINKING WATER QUALITY MONITORING AT PDAM TIRTA", *BAREKENG: J. Math. & App.*, vol. 20, no. 2, pp. 1513-1526, Jun, 2026.

Journal homepage: *https://ojs3.unpatti.ac.id/index.php/barekeng/*
Journal e-mail: *barekeng.math@yahoo.com; barekeng.journal@mail.unpatti.ac.id*

Research Article · **Open Access**

1. INTRODUCTION

Clean water plays a vital role in sustaining ecosystems and safeguarding public health. The availability of water that meets quality standards is a fundamental necessity for daily life as well as for the continuity of various human activities [1]. To ensure this, the Indonesian government has established drinking water quality requirements through the Minister of Health Regulation Number 492/KEMENKES/PER/IV/2010 [2], which must be met by all water service providers, including regional water companies (PDAM). However, natural conditions and infrastructure limitations remain significant challenges in many regions [3]. The Indonesian Ministry of Public Works and Public Housing [4] reported that only about 72% of PDAMs nationwide consistently meet drinking water quality standards, with turbidity and residual chlorine being among the most frequently problematic parameters. In South Sulawesi, seasonal rainfall often causes spikes in turbidity beyond acceptable limits, while residual chlorine levels fluctuate due to dosing and operational challenges, highlighting the urgent need for more reliable monitoring systems [4].

Systematic water quality control is essential to ensure that distributed water consistently meets health requirements [5]. Statistical quality control methods are widely applied to monitor process stability and detect deviations that require corrective action [6]. One of the most common tools in this framework is the control chart, which enables the detection of shifts [7]. However, conventional charts such as the Shewhart chart are effective for detecting large, sudden shifts, while Hotelling's T^2 charts, though widely used for multivariate monitoring, are less sensitive to small or gradual changes [8]. To address these limitations, the Multivariate Exponentially Weighted Moving Average (MEWMA) chart has become increasingly relevant for monitoring multiple quality parameters simultaneously [9]. Unlike traditional charts, MEWMA accumulates historical information through exponential weighting, thereby enhancing sensitivity to small shifts in the process mean while remaining robust when handling data that deviates from perfect normality [10][11].

Several studies have applied MEWMA control charts in the context of water quality monitoring. Maharani et al. [1] implemented MEWMA and MEWMV charts to monitor water treatment quality at PDAM Tirta Moedal, Semarang. Abubakar [4] employed MEWMA charts for water quality monitoring and demonstrated their effectiveness in detecting multivariate shifts in quality parameters. Similarly, Angelita and Pratama [12] applied MEWMA charts to monitor clean water usage at Perumda Tirta Manuntung, Balikpapan. These studies confirm the practical relevance of MEWMA in water-related applications. However, a fundamental limitation of the MEWMA framework lies in its underlying assumption of independent and identically distributed (i.i.d.) observations. In reality, water quality data are collected as time series and often exhibit strong autocorrelation across successive observations. Ignoring this temporal dependence can lead to inflated false alarm rates or failure to detect actual process shifts, thereby reducing the reliability of monitoring outcomes [13][14].

To address this limitation, time series models such as the Vector Autoregressive (VAR) model are widely used because they capture dynamic interdependencies among variables and produce residuals free from autocorrelation. Incorporating these residuals into the MEWMA framework enhances sensitivity to small shifts while minimizing false alarms, thus strengthening the robustness of water quality monitoring systems [13]. Pan and Jarrett [15] demonstrated that incorporating VAR residuals into Hotelling's T^2 charts improved detection reliability by reducing bias caused by serial correlation. Similarly, Khusna [13] developed a VAR-based Max-MCUSUM chart for the white crystal sugar industry and found it more sensitive to small shifts than conventional charts. Building on these findings, the present study proposes a novel approach by integrating VAR residuals into the MEWMA framework for water quality monitoring. Unlike earlier research that primarily focused on T^2 charts or Max-MCUSUM, this study leverages MEWMA's unique advantage in detecting small shifts, thereby enabling earlier identification of process deviations while simultaneously reducing the likelihood of false alarms.

The main objective of this research is to design and implement a VAR-based MEWMA control chart for monitoring water quality at PDAM Tirta Jeneberang, Gowa Regency. By using autocorrelation-free VAR residuals as inputs, this approach is expected to provide a more accurate representation of multivariate water quality dynamics, allow earlier detection of subtle process shifts, and improve both the reliability and efficiency of monitoring systems. The expected outcome is a monitoring framework that ensures timely and accurate detection of process changes while reducing false alarms. Furthermore, this method can serve as a model for other regional water service providers and contribute to the development of multivariate quality control methodologies based on time series analysis, ensuring the sustainable provision of safe and clean drinking water.

2. RESEARCH METHODS

2.1 Vector Autoregressive (VAR)

The Vector Autoregressive (VAR) model is a widely used method in multivariate time series analysis, designed to capture and model autocorrelation relationships among variables within a system. This model is particularly effective in addressing autocorrelation problems that frequently arise in multivariate data [16]. In general, the VAR(p) model can be expressed as follows in Eq.(1):

$$\boldsymbol{X_t} = \boldsymbol{\Phi_1 X_{t-1}} + \boldsymbol{\Phi_2 X_{t-2}} + \cdots + \boldsymbol{\Phi_p X_{t-p}} + \boldsymbol{\varepsilon_t}, \tag{1}$$

where $\boldsymbol{X_t}$ is a $k \times 1$ vector of variables at time t, $\boldsymbol{\Phi_j} = \boldsymbol{\Phi_1, \Phi_2, \ldots, \Phi_n}$ are $k \times k$ vector of VAR coefficient matrices, and $\boldsymbol{\varepsilon_t}$ is a residual vector assumed to follow $\boldsymbol{\varepsilon_t} \sim N(\boldsymbol{0}, \boldsymbol{\Sigma})$. Determining the optimal lag length is a critical step in VAR modeling to ensure reliable parameter estimation and accurate forecasting. In this study, the lag length is determined using the Akaike Information Criterion (AIC), where the model with the smallest AIC value is selected as the most appropriate specification [17][18]. The estimated residuals $\hat{\boldsymbol{\varepsilon}}_{\boldsymbol{t}}$ are subsequently incorporated into the MEWMA statistic for further monitoring analysis.

2.2 VAR-Based Multivariate Exponentially Weighted Moving Average (MEWMA) Control Chart

The Multivariate Exponentially Weighted Moving Average (MEWMA) control chart is an effective statistical method for detecting small shifts in the mean of multivariate processes [19]. By incorporating historical information from previous observations, MEWMA is more sensitive to gradual or subtle changes that may not be immediately apparent [20]. In multivariate systems with temporal dependence, the VAR model is commonly applied to capture dynamic relationships and lagged effects among variables. Once the VAR model is estimated, the residuals $(\hat{\boldsymbol{\varepsilon}}_{\boldsymbol{t}})$ are obtained, representing deviations between observed and predicted values. These residuals serve as critical inputs for the MEWMA procedure [15].

The MEWMA chart then monitors the internal dynamics of the system by accumulating deviations over time, providing early detection of shifts or instability that might be missed by traditional methods [7]. By applying residuals from the VAR model, the MEWMA method accounts for temporal interdependencies while enhancing sensitivity to structural changes. The recursive VAR-Based MEWMA statistic at any time t is defined as Eq. (2):

$$\boldsymbol{Z_t} = \boldsymbol{\Lambda}\hat{\boldsymbol{\varepsilon}}_{\boldsymbol{t}} + (\boldsymbol{I} - \boldsymbol{\Lambda})\boldsymbol{Z_{t-1}}, \qquad \boldsymbol{Z_0} = \boldsymbol{0}, \tag{2}$$

where $\boldsymbol{\Lambda} = \mathrm{diag}(\lambda_1, \lambda_2, \ldots, \lambda_p)$ is a diagonal matrix of smoothing parameters. The general vector representation of $\boldsymbol{Z_t}$ is shown in Eq. (3):

$$\boldsymbol{Z_t} = \begin{bmatrix} \boldsymbol{Z_{11}} & \boldsymbol{Z_{12}} & \cdots & \boldsymbol{Z_{1p}} \\ \boldsymbol{Z_{21}} & \boldsymbol{Z_{22}} & \cdots & \boldsymbol{Z_{2p}} \\ \vdots & \vdots & \ddots & \vdots \\ \boldsymbol{Z_{n1}} & \boldsymbol{Z_{n2}} & \cdots & \boldsymbol{Z_{np}} \end{bmatrix}. \tag{3}$$

In general, the MEWMA observation vector can be expressed as Eq. (4):

$$\boldsymbol{Z_t} = \boldsymbol{\Lambda} \sum_{j=0}^{t-1} (\boldsymbol{I} - \boldsymbol{\Lambda})^{\boldsymbol{j}} \hat{\boldsymbol{\varepsilon}}_{\boldsymbol{t-j}}. \tag{4}$$

Process monitoring is based on Hotelling's statistic in Eq. (5):

$$T_t^2 = \boldsymbol{Z_t'} \boldsymbol{\Sigma}_{\boldsymbol{Z_t}}^{-\boldsymbol{1}} \boldsymbol{Z_t}, \tag{5}$$

where $\boldsymbol{\Sigma}_{\boldsymbol{Z_t}}$ is the covariance matrix of $\boldsymbol{Z_t}$. The variance of $\boldsymbol{Z_t}$ is given by Eq. (6):

$$\boldsymbol{\Sigma}_{\boldsymbol{Z_t}} = \boldsymbol{\Lambda} \left(\sum_{j=0}^{t-1} (\boldsymbol{I} - \boldsymbol{\Lambda})^{2j} \right) \boldsymbol{\Sigma} \boldsymbol{\Lambda}. \tag{6}$$

Using the geometric series expansion, as $t \to \infty$, this converges to Eq. (7):

$$\hat{\boldsymbol{\Sigma}}_{\boldsymbol{Z_t}} = \boldsymbol{\Lambda}(2\mathbf{I} - \boldsymbol{\Lambda})^{-1} \hat{\boldsymbol{\Sigma}} \boldsymbol{\Lambda}. \tag{7}$$

The residual covariance $\hat{\boldsymbol{\Sigma}}$ is estimated by Maximum Likelihood Estimation (MLE) as in Eq. (8):

$$\hat{\boldsymbol{\Sigma}} = \frac{1}{T-p} \sum_{t=p+1}^{T} \hat{\boldsymbol{\varepsilon}}_t \hat{\boldsymbol{\varepsilon}}_t{}' . \tag{8}$$

Under the in-control condition, the test statistic T_t^2 asymptotically follows a chi-square distribution with k degrees of freedom. Thus, the control limits are defined as Eq. (9):

$$LCL = 0, \qquad UCL = \chi^2_{k,\alpha}, \tag{9}$$

where α is the chosen significance level. If $T_t^2 > UCL$, the process is signaled as out-of-control, indicating a potential deviation or shift in the process mean. Such signals imply significant changes in the system that may require corrective action to restore stability. The ability of the VAR-based MEWMA approach to provide early detection of such changes is crucial for maintaining process quality and preventing adverse outcomes.

2.3 Analysis Method

The analytical procedure in this study was carried out through several structured steps. First, descriptive statistics were applied to the 2023 daily dataset, which consisted of 365 observations of turbidity (NTU) and residual chlorine (mg/L) to identify patterns, fluctuations, and potential outliers. Next, a VAR model was constructed, with the optimal lag order determined using the AIC. The model parameters were then estimated using the OLS method and validated through a residual autocorrelation test (Portmanteau test) and causality tests (Granger and instantaneous causality) to evaluate the interrelationships between variables. The VAR residuals, calculated as the difference between actual and predicted values, were subsequently used as inputs for the Residual-based MEWMA control chart. To ensure that the fundamental assumptions of MEWMA were satisfied, a multivariate normality test was conducted using the Mahalanobis distance compared against the Chi-Square distribution. The smoothing parameter (λ) was evaluated over a range of 0.01 to 0.9 based on three criteria: the number of out-of-control points, the smallest difference between the maximum T_t^2 value and UCL, and the minimum average distance of T_t^2 values to UCL. Finally, the standard MEWMA chart and the VAR-based MEWMA chart were compared to assess their relative effectiveness in detecting changes in water quality. All stages of data processing, model estimation, and simulation were performed using the software R.

3. RESULTS AND DISCUSSION

The application of the VAR-based MEWMA control chart for water quality monitoring in this study focuses on two key parameters that PDAM must continuously supervise: turbidity and residual chlorine. According to drinking water standards, turbidity should not exceed 5 NTU to prevent the presence of particles that may carry microorganisms or contaminants, while residual chlorine (Cl_2) should remain below 0.5 mg/L to ensure effective disinfection without excessive chlorination. Monitoring these parameters is therefore essential to guarantee that the supplied water remains safe and compliant with public health regulations. The dataset used in this study consists of 365 daily observations collected from January 1 to December 31, 2023, providing a comprehensive picture of the annual dynamics of water quality. Descriptive statistics and graphical summaries for turbidity (NTU) and residual chlorine (mg/L) are presented in Figure 1, which illustrates the temporal distribution of both variables.

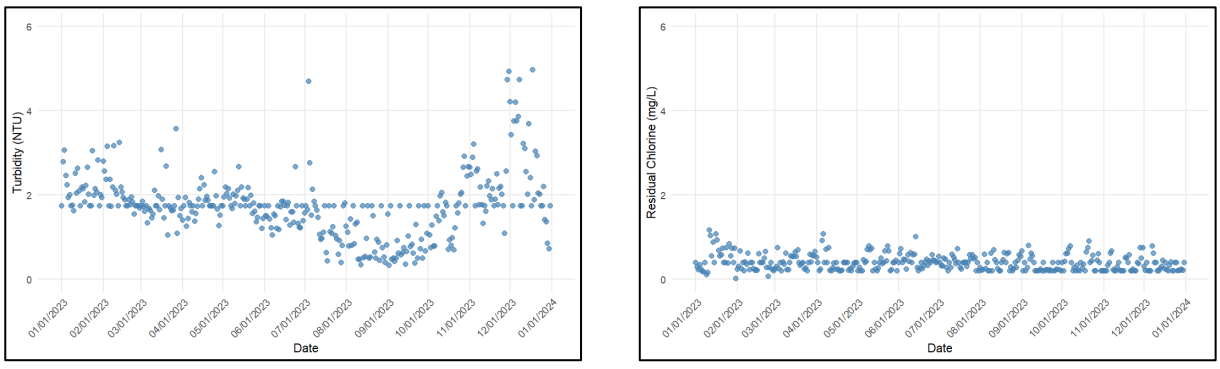

(a) **(b)**

Figure 1. (a) Turbidity Data Distribution (NTU), (b) Residual Chlorine Data Distribution (mg/L)

The descriptive statistical analysis of water quality data for 2023, as shown in Figure 1, highlights noticeable fluctuations in turbidity and residual chlorine throughout the year. The highest average turbidity level was recorded in December at 2.60 NTU, while the lowest occurred in September at 0.88 NTU. For residual chlorine, the highest monthly average was observed in January at 0.52 mg/L, whereas the lowest averages were found in September and December, each at 0.31 mg/L. Fluctuations in these parameters, particularly the significant increases in December (turbidity) and January (residual chlorine), suggest instability in water quality. These variations are likely caused by seasonal factors such as increased rainfall and operational challenges in the water treatment system during these months, which can affect the effectiveness of water purification processes and contribute to changes in water quality.

Beyond these monthly variations, the graphs also reveal the presence of extreme values (outliers) that deviate significantly from the general data pattern. In the turbidity graph, several points in December approach or even exceed 5 NTU, which is the maximum allowable threshold for drinking water quality. This indicates specific events that caused sudden increases in suspended particles, most likely due to heavy rainfall or disruptions in the filtration process. Meanwhile, in the residual chlorine graph, several extreme points are observed in early 2023 (January–February), with concentrations exceeding 1.0 mg/L, clearly above the recommended limit of 0.5 mg/L. These spikes may indicate periods of over-chlorination, possibly undertaken as a response to increased microbial loads in the raw water.

The presence of these outliers is important from an operational perspective, as they do not merely reflect natural variability but may also signal process disturbances or extreme environmental conditions that threaten the stability of the PDAM treatment system. This underlines the need for monitoring tools that can detect such abnormal behavior at an early stage. In this context, the VAR-based MEWMA control chart complements conventional descriptive analysis by offering higher sensitivity to abnormal changes and providing a structured framework for distinguishing random fluctuations from potential process shifts.

3.1 Determination of The Optimal VAR Lag

Determining the optimal lag order in a VAR model is a crucial step for achieving an appropriate model specification, as lag selection directly affects both the accuracy and stability of the resulting model. An insufficient lag order may fail to capture the underlying dynamics, whereas an excessively large lag order can lead to overparameterization and loss of efficiency. In this study, the optimal lag length is determined using the Akaike Information Criterion (AIC), which balances goodness of fit against model complexity.

Table 1. Optimal Lag Selection for The VAR Model

Lag	AIC
1	- 4.355
2	- 4.428
3	- 4.478
4	- 4.475
5	- 4.469

Table 1 shows that the lowest AIC value is obtained at lag 3, with a score of –4.478. Based on the AIC criterion, the model with the smallest value is considered optimal, as it provides the best trade-off between goodness of fit and model parsimony. Accordingly, lag 3 was selected as the optimal lag for the VAR model to ensure more reliable and accurate parameter estimation. Therefore, all subsequent analyses in this study are carried out using the VAR(3) model.

3.2 Parameters Estimation of The VAR Model

Once the optimal lag order has been determined, the next step is to estimate the parameters of the VAR model. Parameter estimation is essential for quantifying the dynamic interactions among variables and assessing the statistical significance of lagged effects. In this study, the parameters of the VAR model are estimated using the Ordinary Least Squares (OLS) method, which provides consistent and unbiased estimators for each equation in the system when the lag order is correctly specified. The analysis focuses on the joint dynamics of two main water quality indicators, turbidity and residual chlorine, modeled within the VAR(3) framework. As shown in Table 1, the optimal lag length was determined to be lag 3 based on the lowest AIC value.

Table 2. Estimation of VAR(3) Model Parameters for the Residual Turbidity Variable

Variable	Estimate	Std. Error	T-Value	P-Value
Constant	0.334	0.120	2.787	0.006
Turbidity Lag 1	0.354	0.052	6.860	0.000*
Residual Chlorine Lag 1	0.038	0.173	0.219	0.827
Turbidity Lag 2	0.172	0.055	3.146	0.002*
Residual Chlorine Lag 2	0.080	0.182	0.440	0.661
Turbidity Lag 3	0.250	0.052	4.824	0.000*
Residual Chlorine Lag 3	0.008	0.173	0.047	0.963

Based on the estimation results in Table 2, the VAR(3) model for the turbidity variable can be expressed as:

$$x_{1,t} = 0.334 + 0.354x_{1,t-1} + 0.038x_{2,t-1} + 0.172x_{1,t-2} + 0.080x_{2,t-2} + 0.250x_{1,t-3} + 0.008x_{2,t-3}.$$

The coefficients of turbidity at lags 1, 2, and 3 are all statistically significant at the 5% level (p-value < 0.05), indicating that turbidity from the previous three periods exerts a strong and persistent influence on current turbidity levels. In contrast, the coefficients of residual chlorine at lags 1, 2, and 3 are not statistically significant (p-value > 0.05), suggesting that residual chlorine does not have a meaningful lagged impact on turbidity in this model. Overall, these results highlight that turbidity dynamics are primarily driven by their own past values, rather than by lagged effects of chlorine residual. This implies that the temporal persistence of turbidity is the dominant factor in explaining its current fluctuations.

Table 3. Estimation of VAR(3) Model Parameters for the Residual Chlorine Variable

Variable	Estimate	Std. Error	T-Value	P-Value
Constant	0.250	0.037	6.789	0.000*
Turbidity Lag 1	-0.024	0.016	-1.517	0.130
Residual Chlorine Lag 1	0.341	0.053	6.401	0.000*
Turbidity Lag 2	0.014	0.017	0.858	0.391
Residual Chlorine Lag 2	0.138	0.056	2.481	0.014*
Turbidity Lag 3	-0.002	0.016	-0.096	0.924
Residual Chlorine Lag 3	-0.068	0.053	-1.283	0.200

Based on the estimation results in Table 3, the VAR(3) model for residual chlorine can be expressed as:

$$x_{2,t} = 0.250 - 0.024x_{1,t-1} + 0.341x_{2,t-1} + 0.014x_{1,t-2} + 0.138x_{2,t-2} - 0.002x_{1,t-3} - 0.068x_{2,t-3}.$$

The constant term is highly significant (p-value = 0.000), indicating its strong contribution to the model. Residual chlorine at lag 1 is also highly significant (p-value = 0.000), showing that current residual chlorine levels are strongly influenced by the previous day's value. Residual chlorine at lag 2 is significant at the 5% level (p-value = 0.014), suggesting a continued effect from two days earlier. By contrast, neither turbidity lag nor residual chlorine at lag 3 is statistically significant (p-value > 0.05), indicating that turbidity does not play a significant lagged role in determining residual chlorine dynamics in this specification. These findings imply that residual chlorine behavior is mainly driven by its own past values, particularly at lags 1 and 2, whereas turbidity has no substantial lagged effect on the chlorine equation.

3.3 Residual Autocorrelation Test for The VAR Model

The residual autocorrelation test is essential to ensure that the residuals from the VAR model are not correlated with their own past values or with the residuals of other variables. The presence of autocorrelation would indicate that the model has not fully captured the underlying dynamics of the data, potentially undermining the validity of the parameter estimates. To examine this, the Portmanteau test was employed, as it can detect residual autocorrelation simultaneously across multiple lags. In this study, the test was conducted using daily data for one year, and the lag length was extended up to lag 30 to capture potential short- and medium-term autocorrelation patterns, including weekly or monthly cycles that may exist in the data.

Table 4. Results of the Residual Autocorrelation Test (Portmanteau Test)

Chi-Square	Degrees of Freedom (df)	P-Value
113.360	108	0.055

Based on Table 4, the results show that the Portmanteau test statistic is 113.360 with 108 degrees of freedom and a p-value of 0.055. Since the p-value is greater than the 5% significance level, this indicates that there is no significant residual autocorrelation up to lag 30. Hence, the VAR model satisfies the no-autocorrelation assumption, and the parameter estimates can be considered valid.

3.4 Causality Test for The VAR Model

Causality testing was then conducted to examine the directional relationships between turbidity and residual chlorine within the VAR framework. Two approaches were applied: Granger causality, which evaluates whether past values of one variable can statistically predict another, and instantaneous causality, which tests for contemporaneous causal relationships occurring at the same time.

Table 5. Results of Causality Tests Between Turbidity and Residual Chlorine

Causal Direction	Test Type	Test Statistic	P-Value
Turbidity → Residual Chlorine	Granger Causality	F = 2.314	0.025
Residual Chlorine → Turbidity	Granger Causality	F = 1.024	0.413
Turbidity ↔ Residual Chlorine	Instantaneous Causality	χ^2 = 6.420	0.011

The results in Table 5 indicate that turbidity has a causal effect on residual chlorine according to the Granger causality test, with a p-value of 0.025 (< 0.05). Thus, there is evidence of a one-way causal relationship from turbidity to residual chlorine. In contrast, the reverse direction (residual chlorine → turbidity) is not statistically significant (p-value = 0.413 > 0.05), suggesting that residual chlorine does not help predict changes in turbidity. Furthermore, the instantaneous causality test yields a significant result with a p-value of 0.011, indicating the presence of a direct and simultaneous causal relationship between turbidity and residual chlorine. This suggests that fluctuations in the two variables may occur concurrently, reflecting systemic interdependence in the water treatment process.

3.5 Formation of Residuals from The VAR Model

After determining the optimal VAR order based on the AIC criterion, the model parameters for turbidity and residual chlorine were estimated. The residuals were then calculated as the difference between the actual observed values $\boldsymbol{X_t}$ and the predicted values $\widehat{\boldsymbol{X}}_{\boldsymbol{t}}$ from the VAR model at each time point, as expressed in Eq. (10).

$$\hat{\boldsymbol{\varepsilon}}_{\boldsymbol{t}} = \boldsymbol{X_t} - \widehat{\boldsymbol{X}}_{\boldsymbol{t}}. \tag{10}$$

These residuals represent the random components of the process after accounting for temporal dependencies among the variables. They are used as inputs to the MEWMA control chart, since residuals are assumed to be relatively free from autocorrelation, thereby better satisfying the independence assumption.

Table 6. Residuals from The VAR Model for Turbidity and Residual Chlorine

Time (t)	Turbidity (ε_{1t})	Residual Chlorine (ε_{2t})
1	0.095	0.038
2	-0.228	-0.117
3	-0.409	-0.161
4	-0.047	-0.133
5	-0.215	0.097
⋮	⋮	⋮
360	-0.784	-0.091
361	-0.528	-0.130
362	0.637	0.058

The results in Table 6 show that both turbidity and chlorine residuals fluctuate between positive and negative values. Positive residuals imply that the VAR model underestimated the actual value, while negative residuals indicate overestimation. For instance, at time $t = 3$, the turbidity residual of -0.409 suggests that the model prediction was higher than the observed value. The extreme value may serve as an early warning indicator of potential out-of-control conditions in the MEWMA chart.

Overall, turbidity residuals exhibit higher variability and more frequent fluctuations compared to residual chlorine, which remains relatively stable and mostly below 1 throughout the observation period. Significant spikes in turbidity residuals are particularly evident in early August 2023 and become more pronounced from October to December 2023, with several values exceeding 4. This pattern suggests anomalies or operational disturbances in the water treatment process that were not fully captured by the VAR model. In contrast, residual chlorine appears more stable, although small spikes are occasionally observed. The period from October to December 2023 can therefore be considered critical, as consistent increases in turbidity residuals indicate potential deterioration in treatment performance. These spike points will be of particular concern when constructing the MEWMA control chart, as they are likely to exceed the upper control limit and generate out-of-control signals.

3.6 Multivariate Normality Test for MEWMA Control Chart

The multivariate normality test was conducted to verify whether the variables used in the model jointly follow a multivariate normal distribution. This assumption is one of the key requirements for the application of the VAR-based MEWMA control chart. In this study, the Mahalanobis distance approach was applied and compared with the Chi-Square distribution. The dataset consists of two variables observed over one year, namely the residuals of turbidity and residual chlorine, with dimensionality $\boldsymbol{p = 2}$ and a total of $\boldsymbol{T = 362}$ observations. The Mahalanobis distance for each observation was calculated using Eq. (11). These values were then compared with the Chi-Square quantiles at $\boldsymbol{df = 2}$. The comparison results are presented in Table 7.

$$\boldsymbol{d_t^2 = (\varepsilon_t - \bar{\varepsilon})' \hat{\Sigma}^{-1} (\varepsilon_t - \bar{\varepsilon})}. \quad \textbf{(11)}$$

Table 7. Results of Multivariate Normality Test

Time (t)	d_t^2	χ^2	Description
1	0.000	0.003	$d_1^2 \leq \chi^2$
2	0.000	0.008	$d_2^2 \leq \chi^2$
3	0.000	0.014	$d_3^2 \leq \chi^2$
4	0.000	0.019	$d_4^2 \leq \chi^2$
5	0.000	0.025	$d_5^2 \leq \chi^2$
⋮	⋮	⋮	
360	16.600	9.967	$d_{360}^2 > \chi^2$
361	18.669	10.989	$d_{361}^2 > \chi^2$
362	19.765	13.186	$d_{362}^2 > \chi^2$

The results in Table 7 show that 338 out of 362 observations (approximately 93.4%) satisfy the criterion $\boldsymbol{d_t^2 \leq \chi^2}$. Since this proportion is well above 50%, it can be concluded that the water quality characteristics of PDAM Tirta Jeneberang reasonably follow a multivariate normal distribution. This finding is further illustrated in the Mahalanobis distance versus Chi-Square quantile plot shown in Figure 2. Most points lie close to the diagonal line, indicating good agreement with the multivariate normal distribution, although a few points deviate in the tail region, suggesting the presence of some extreme observations. With the multivariate normality assumption reasonably satisfied, the MEWMA analysis can be applied more reliably, and the resulting control charts can be interpreted with greater confidence.

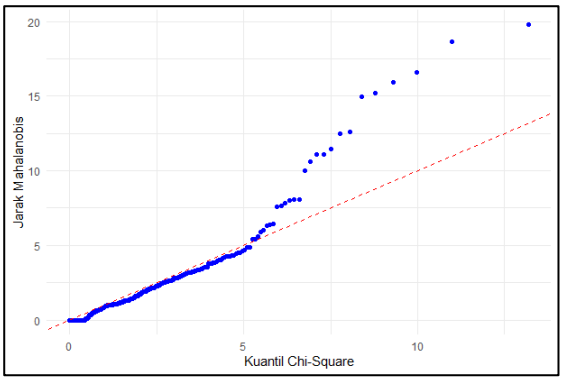

Figure 2. Mahalanobis Distance vs Chi-Square Quantile Plot

3.7 Determination of Smoothing Parameter for MEWMA Control Chart

The selection of the smoothing parameter (λ) is a critical step in constructing the MEWMA control chart, as it directly affects the sensitivity and stability of the system in detecting process shifts. A very small value of λ may result in slow responses to disturbances, while an excessively large value can make the chart overly sensitive to natural variation (noise), thereby increasing the likelihood of false alarms. In this study, ten different values of λ ranging from 0.01 to 0.9 were evaluated. Each value was selected based on:

1. Number of out-of-control points, calculated as the number of observations that exceed the UCL for each smoothing parameter. A higher count indicates greater sensitivity of the system to small process shifts.
2. Smallest difference between the maximum $\boldsymbol{T_t^2}$ value and the UCL, which reflects how close the largest deviation is to the control limit. A smaller difference suggests better stability in detecting process changes.
3. Minimum average distance of $\boldsymbol{T_t^2}$ values to the UCL, representing the overall consistency of the monitoring system. A lower average distance indicates a more stable and reliable detection mechanism.

Table 8. Evaluation of Smoothing Parameter in MEWMA Control Chart

Smoothing Parameter ($\boldsymbol{\lambda}$)	Maximum T^2 Value	UCL	Out of Control Point	Difference (Max T^2 – UCL)	Average Distance to UCL
0.01	6.030	5.991	2	0.039	3.910
0.02	8.791	5.991	33	2.799	3.699
0.03	**11.295**	**5.991**	**41**	**5.304**	**3.835**
0.05	15.074	5.991	39	9.083	4.103
0.08	16.526	5.991	28	10.535	4.757
0.1	16.582	5.991	26	10.591	4.446
0.2	24.649	5.991	24	18.658	4.655
0.3	30.156	5.991	21	24.165	4.714
0.5	32.436	5.991	20	26.445	4.763
0.9	28.233	5.991	19	22.242	4.728

Table 8 shows that when $\boldsymbol{\lambda = 0.01}$, only 2 out-of-control points were detected, indicating that the system was too slow to respond to small process changes. Conversely, at $\boldsymbol{\lambda = 0.03}$, the number of out-of-control points reached the highest value of 41, suggesting that this setting is highly sensitive to small deviations. The maximum deviation at $\boldsymbol{\lambda = 0.03}$ (5.304) remains within a reasonable range, and the average distance to the UCL (3.835) is relatively stable compared to other values. At higher values of $\boldsymbol{\lambda}$ (e.g., 0.30 and 0.50), although the difference between the maximum $\boldsymbol{T_t^2}$ and the UCL is larger (24.165–26.445), the number of out-of-control points decreases significantly (20–21 points). This indicates that the system loses sensitivity to smaller shifts despite detecting large deviations. Considering the balance between detection sensitivity and monitoring stability, $\boldsymbol{\lambda = 0.03}$ is selected as the most optimal smoothing parameter. This

value effectively detects small process changes without generating excessive false alarms, making it well-suited for the application of the VAR-based MEWMA control chart in monitoring the water quality of PDAM Tirta Jeneberang.

3.8 Monitoring of VAR-Based MEWMA and MEWMA Standard Control Charts

After determining the optimal smoothing parameter at $\boldsymbol{\lambda = 0.03}$, monitoring of water quality at PDAM Tirta Jeneberang was carried out using the VAR-based MEWMA control chart. The monitoring results are presented in Figure 3.

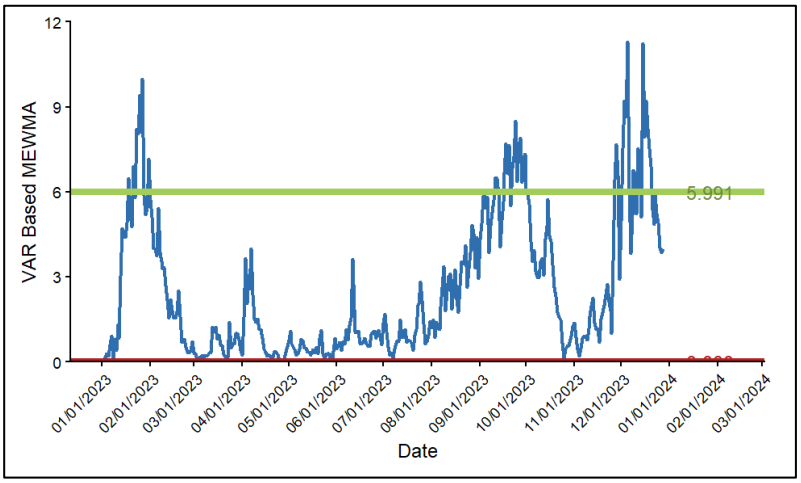

Figure 3. VAR-Based MEWMA Control Chart

The UCL was set at 5.991 based on the Chi-Square distribution with two degrees of freedom at the 5% significance level ($\chi^2_{2,0.05} = 5.991$), while the LCL was fixed at 0 because the T_t^2 statistic cannot take negative values. The results indicate substantial fluctuations of T_t^2 throughout 2023, with several spikes exceeding the UCL. These occurred primarily in early February, mid-year (June–September), and reached their peak during November–December, suggesting that the final quarter of the year represents a critical period for process stability.

A total of 41 out-of-control points were identified. Some of these signals are likely associated with actual water quality issues, such as increased turbidity due to heavy rainfall or disturbances in the disinfection process, particularly during the end of the year (December). Nevertheless, without direct verification against PDAM's operational records, the practical significance of these detections cannot be fully ascertained. The observed deviations may be attributed to seasonal effects, plant maintenance activities, or operational errors such as inaccuracies in chemical dosing. In addition, some of the points may represent false positives caused by random fluctuations or model limitations, while others constitute true signals of quality violations. Therefore, integrating statistical monitoring results with operational data is essential to more accurately distinguish between valid signals and false alarms, thereby ensuring that the monitoring outcomes provide optimal support for decision-making.

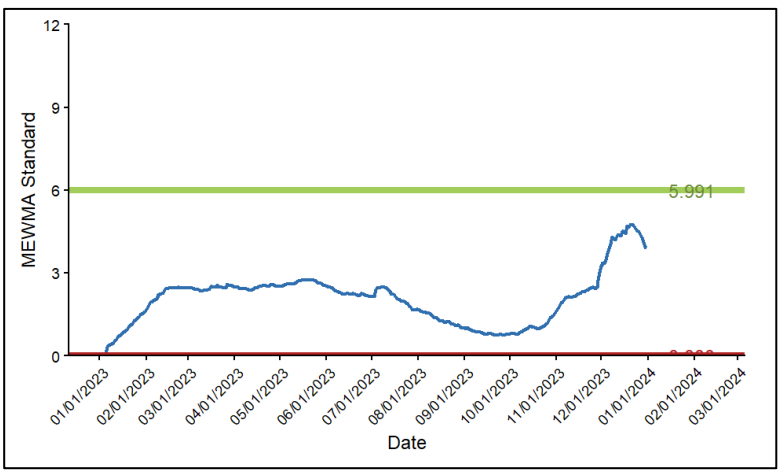

Figure 4. Standard MEWMA Control Chart

To evaluate the effectiveness of the proposed approach, a comparison was conducted with the standard MEWMA control chart, as presented in Figure 4. The standard MEWMA chart, which was constructed directly from raw turbidity and residual chlorine data without accounting for temporal dependence, exhibited a relatively smoother and more stable pattern. Throughout the observation period, all T_t^2 values remained below the UCL, suggesting that the process appeared to be under control. However, this finding also highlights a key limitation of the standard MEWMA, namely its lack of sensitivity in detecting small shifts or hidden anomalies within the system. In contrast, the VAR-based MEWMA control chart demonstrated greater responsiveness in capturing process variability. By utilizing the residuals from the VAR model, which incorporate temporal dynamics and interdependencies between variables, the control chart was able to detect deviations that were not visible in the standard MEWMA chart. The out-of-control points identified in Figure 3 revealed significant process instabilities and shifts, particularly during the latter months of 2023, which went undetected by the conventional approach.

Overall, the comparison confirms that the VAR-based MEWMA control chart offers superior sensitivity in detecting both small and large process shifts, while also uncovering hidden anomalies that the standard MEWMA fails to identify. These findings emphasize that the VAR-based MEWMA provides a more reliable and suitable monitoring tool for the multivariate and dynamic characteristics of water quality processes at PDAM Tirta Jeneberang. From a practical perspective, the integration of the VAR-based MEWMA chart can serve as an early warning system, enabling PDAM to undertake timely operational interventions to prevent water quality deterioration that may pose risks to public health.

3.9 Comparison of Average Run Length (ARL)

The Average Run Length (ARL) is a key metric for evaluating the performance of control charts, defined as the average number of observations until the first signal occurs. The ARL_0 (in-control) represents the chart's stability under normal conditions, where larger ARL_0 values indicate fewer false alarms. Conversely, ARL_1 (out-of-control) measures detection speed when a mean shift occurs, with smaller ARL_1 values reflecting faster signaling. In this study, we compare the performance of the standard MEWMA chart and the VAR-based MEWMA chart, using parameters $\boldsymbol{\lambda = 0.03}$ and UCL = 5.991. The standard MEWMA chart was constructed using the covariance of raw data, while the VAR-based MEWMA utilized residuals from the VAR(3) model, which are free from autocorrelation. Monte Carlo simulations with 5,000 replications were conducted across three scenarios: S_1 (shift in turbidity), S_2 (shift in residual chlorine), and S_3 (simultaneous shift in both), with shift magnitudes $\boldsymbol{\delta \in \{0.25, 0.5, 0.75, \ldots, 2.0\}}$.

Table 9. Comparison of ARL between MEWMA Standard vs VAR-based MEWMA

Scenario	Shift Magnitudes (δ)	ARL_0		ARL_1	
		MEWMA Standard	VAR Based MEWMA	MEWMA Standard	VAR Based MEWMA
S_1: shift Turbidity	0.25	3.026	3.006	2.828	2.732
	0.50	3.026	3.006	2.550	2.136
	0.75	3.026	3.006	2.179	1.738
	1.00	3.026	3.006	1.866	1.447
	1.25	3.026	3.006	1.639	1.267
	1.50	3.026	3.006	1.480	1.138
	1.75	3.026	3.006	1.334	1.057
	2.00	3.026	3.006	1.231	1.023
S_2: shift Residual Chlorine	0.25	3.016	3.003	1.738	1.640
	0.50	3.016	3.003	1.137	1.091
	0.75	3.016	3.003	1.009	1.004
	1.00	3.016	3.003	1.000	1.000
	1.25	3.016	3.003	1.000	1.000
	1.50	3.016	3.003	1.000	1.000
	1.75	3.016	3.003	1.000	1.000
	2.00	3.016	3.003	1.000	1.000

Scenario	Shift Magnitudes (δ)	ARL_0		ARL_1	
		MEWMA Standard	VAR Based MEWMA	MEWMA Standard	VAR Based MEWMA
S_3: shift Turbidity and Residual Chlorine	0.25	3.009	2.983	1.719	1.634
	0.50	3.009	2.983	1.124	1.089
	0.75	3.009	2.983	1.008	1.002
	1.00	3.009	2.983	1.000	1.000
	1.25	3.009	2.983	1.000	1.000
	1.50	3.009	2.983	1.000	1.000
	1.75	3.009	2.983	1.000	1.000
	2.00	3.009	2.983	1.000	1.000

The results in Table 9 show that both methods yield comparable ARL_0 values (approximately 3) across all scenarios, indicating that the use of VAR residuals does not increase the false alarm frequency under in-control conditions. Clear differences, however, emerge in ARL_1, particularly in Scenario S1 involving shifts in turbidity. For all δ values, the VAR-based MEWMA consistently produces smaller ARL_1 values than the standard MEWMA, indicating faster detection of process shifts. For example, at $\delta = 1.0$, ARL_1 decreases from 1.866 (standard MEWMA) to 1.447 (VAR-based MEWMA), corresponding to an improvement of roughly 22%. This advantage reflects the higher volatility and strong autocorrelation structure of turbidity, for which the VAR adjustment is especially effective. By contrast, in Scenarios S_2 (chlorine) and S_3 (turbidity and chlorine), the differences between the two methods are relatively minor and vanish for $\delta \geq 0.75$, as larger shifts are naturally easier to detect regardless of the charting method. Overall, these findings demonstrate that the VAR-based MEWMA achieves more efficient detection of small shifts without compromising ARL_0 stability, particularly for turbidity, a critical parameter in ensuring drinking water quality. This enhanced sensitivity positions the VAR-based MEWMA as a valuable early-warning tool, enabling water utilities to initiate corrective actions more promptly before water quality deteriorates beyond regulatory standards.

4. CONCLUSION

This study developed and applied a VAR-based MEWMA control chart for monitoring turbidity and residual chlorine in drinking water at PDAM Tirta Jeneberang. By incorporating autocorrelation-free residuals from a VAR(3) model into the MEWMA framework with $\lambda = 0.03$, the proposed approach successfully addressed the temporal dependence inherent in daily water quality data. The empirical results showed that both the standard and VAR-based MEWMA charts produced similar ARL_0 values (approximately 3), confirming that the use of VAR residuals does not degrade in-control stability or increase the frequency of false alarms. However, the VAR-based MEWMA consistently achieved lower ARL_1 values, particularly in scenarios involving shifts in turbidity, with improvements of up to 22% compared with the standard MEWMA. These findings indicate that the VAR-based approach is more sensitive to small and gradual process shifts, while still minimizing false alarms.

Overall, the study demonstrates that the VAR-based MEWMA provides a more robust and reliable monitoring tool than the conventional MEWMA chart for autocorrelated multivariate water quality data. It enhances the early detection of subtle deviations, particularly in turbidity, which is a critical parameter for maintaining drinking water safety and can therefore serve as an effective early-warning system to support PDAM operations. Beyond the specific case of PDAM Tirta Jeneberang, the proposed methodology has strong potential for adoption by other regional water utilities and for broader application in time-series-based multivariate quality control, contributing to more proactive and data-driven water supply management.

Author Contributions

Agung Muhammad Takdir: Conceptualization, Methodology, Writing-Original Draft, Software, Validation, Writing-Review and Editing. Erna Tri Herdiani: Data Curation, Resources, Draft Preparation, and Editing. Nurtiti Sunusi: Formal Analysis, Validation, and Editing. All authors discussed the results and contributed to the final manuscript.

Funding Statement

The authors would like to express their sincere gratitude to PDAM Tirta Jeneberang, Gowa Regency, for their valuable support in providing the water quality data used in this study. Their contribution has been essential in enabling the completion of this research.

Acknowledgment

The research team would like to express our deepest gratitude to the individuals and institutions that have made important contributions to the success of our research. The support, guidance, and collaboration provided have been invaluable to the smooth progress and success of this research.

Declarations

The authors declare that there are no conflicts of interest associated with this study. The authors have equally contributed to the design, analysis, and interpretation of the study, and the final manuscript was reviewed and approved by all authors.

Declaration of Generative AI and AI-assisted technologies

ChatGPT was used only to improve the readability and grammatical structure of the manuscript. No AI tool was used to generate or alter the research data, methodology, results, or interpretations. All content was verified by the authors for accuracy and consistency with the study.

REFERENCES

[1] A. A. Maharani, Mustafid, and Sudarno, "PENERAPAN DIAGRAM KONTROL MEWMA DAN MEWMV PADA PENGENDALIAN KARAKTERISTIK KUALITAS AIR (STUDI KASUS: KUALITAS PENGOLAHAN AIR II PDAM TIRTA MOEDAL KOTA SEMARANG)," *Jurnal Gaussian*, vol. 7, no. 1, pp. 23–32, 2018, doi: https://doi.org/10.14710/j.gauss.v7i1.26632

[2] P. de Rozari, I. Nurwiana, and L. L. Leko, "KONDISI KUALITAS AIR DAN PERILAKU MASYARAKAT DI SUB DAERAH ALIRAN SUNGAI (DAS) KALI LILIBA KOTA KUPANG," *Jurnal Inovasi Kebijakan*, vol. 5, no. 2, 2020, doi: https://doi.org/10.37182/jik.v5i2.57

[3] R. Rasyid, E. T. Herdiani, and N. Sunusi, "PETA KENDALI P BERDASARKAN METODE PENINGKATAN TRANSFORMASI AKAR KUADRAT," *ESTIMASI: Journal of Statistics and Its Application*, pp. 27–36, Jan. 2024, doi: https://doi.org/10.20956/ejsa.v5i1.18487

[4] A. Abubakar, "MONITORING KUALITAS AIR DENGAN MENGGUNAKAN BAGAN KENDALI *MULTIVARIATE EXPONENTIALLY WEIGHTED MOVING AVERAGE*," *Jurnal Saintek Patompo*, vol. 1, no. 1, pp. 29–38, 2023, doi: https://doi.org/10.29313/bcss.v3i2.9261

[5] W. Ikhsan, W. Ardytia, and I. K. Soetijino, "IMPLEMENTASI KEBIJAKAN PELESTARIAN LINGKUNGAN HIDUP MELALUI KONSERVASI SUMBER MATA AIR DI GOMBENGSARI KALIPURO BANYUWANGI," *Jurnal Populika*, vol. 9, no. 2, 2021, doi: https://doi.org/10.37631/populika.v9i2.811

[6] D. C. Montgomery, DESIGN AND ANALYSIS OF EXPERIMENTS, 6th Edition. New York: John Wiley & Sons, 2005.

[7] N. K. Y. Dewiantari, I. W. Sumarjaya, and G. K. Gandhiadi, "PETA KENDALI EWMA RESIDUAL PADA DATA BERAUTOKORELASI," *E-Jurnal Matematika*, vol. 8, no. 1, pp. 64–73, Feb. 2019, doi: https://doi.org/10.24843/mtk.2019.v08.i01.p236

[8] J. C. Montgomery, R. G. Wardell, and W. H. Woodall, "AN EVALUATION OF MULTIVARIATE EXPONENTIALLY WEIGHTED MOVING AVERAGE CONTROL CHARTS," Journal of Quality Technology, vol. 31, no. 3, pp. 285–292, 1999.

[9] Irma, D. Anggraini, and F. M. Farid, "PETA KENDALI MULTIVARIAT NP," *RAGAM: Journal of Statistics and Its Application*, vol. 1, no. 1, pp. 1–13, Dec. 2022, doi: https://doi.org/10.20527/ragam.v1i1.7387

[10] I. Antono and R. Santoso, "KOMPUTASI *METODE EXPONENTIALLY WEIGHTED MOVING AVERAGE* UNTUK PENGENDALIAN KUALITAS PROSES PRODUKSI MENGGUNAKAN GUI MATLAB (STUDI KASUS: PT DJARUM KUDUS SKT BRAK MEGAWON III)," *Jurnal Gaussian*, vol. 5, no. 4, pp. 673–682, 2016, doi: https://doi.org/10.14710/j.gauss.v9i3.28908

[11] T. K. Biswas and A. Ghosh, "APPLICATION OF MULTIVARIATE CONTROL CHARTS IN WATER QUALITY MONITORING: A CASE STUDY," *Environmental Monitoring and Assessment*, vol. 192, no. 6, pp. 1–15, 2020.

[12] M. Angelita and A. P. Pratama, "KONTROL PENGGUNAAN AIR BERSIH PERUMDA TIRTA MANUNTUNG BALIKPAPAN DENGAN *MULTIVARIATE EXPONENTIALLY WEIGHTED MOVING AVARAGE*," *SPECTA Journal of Technology*, vol. 7, no. 3, pp. 642–649, 2023.

[13] H. Khusna, M. Mashuri, and Wibawati, "VECTOR AUTOREGRESSIVE-BASED MAXIMUM MCUSUM CONTROL CHART FOR MONITORING THE QUALITY OF WHITE CRYSTAL SUGAR," in *Journal of Physics: Conference Series*, IOP Publishing Ltd, Dec. 2021, doi: https://doi.org/10.1088/1742-6596/2123/1/012034

[14] Z. Zhang, S. Liu, and Y. Wang, "SPATIOTEMPORAL MONITORING OF WATER QUALITY USING MULTIVARIATE STATISTICAL PROCESS CONTROL METHODS," *Water Research*, vol. 145, pp. 703–713, 2018.

[15] X. Pan and J. Jarrett, "USING VECTOR AUTOREGRESSIVE RESIDUALS TO MONITOR MULTIVARIATE PROCESSES IN THE PRESENCE OF SERIAL CORRELATION," *Int J Prod Econ*, vol. 106, no. 1, pp. 204–216, Mar. 2007, doi: https://doi.org/10.1016/j.ijpe.2006.07.002

[16] E. Andini, Sudarno, and R. Rahmawati, "PENERAPAN METODE PENGENDALIAN KUALITAS MEWMA BERDASARKAN ARL DENGAN PENDEKATAN RANTAI MARKOV (STUDI KASUS: BATIK SEMARANG 16, METESEH)," *Jurnal Gaussian*, vol. 10, no. 1, pp. 125–135, 2021, doi: https://doi.org/10.14710/j.gauss.v10i1.30939

[17] A. A.-Z. Nugroho, "PEMODELAN *MULTIVARIATE TIME SERIES* DENGAN *VECTOR AUTOREGRESSIVE INTEGRATED MOVING AVERAGE* (VARIMA)," *Jurnal Riset Statistika*, pp. 93–102, Dec. 2022, doi: https://doi.org/10.29313/jrs.v2i2.1150

[18] R. A. Johnson and D. W. Wichern, *APPLIED MULTIVARIATE STATISTICAL ANALYSIS*, 6th Edition. Pearson Education, 2007.

[19] Y. D. S, B. Pramusintho, F. Firmansyah, and F. Hoesni, "MODEL PERAMALAN HARGA TELUR AYAM RAS DI PASAR TRADISIONAL DAN MODERN KOTA JAMBI," *Ekonomis: Journal of Economics and Business*, vol. 6, no. 1, pp. 372–382, Mar. 2022, doi: https://doi.org/10.33087/ekonomis.v6i1.521

[20] M. B. Saritha and R. Varadharajan, "MULTIVARIATE EXPONENTIALLY WEIGHTED MOVING AVERAGE CONTROL CHART UNDER NEUTROSOPHIC ENVIRONMENT: A BOOTSTRAP APPROACH," *International Journal of Mathematical, Engineering and Management Sciences*, vol. 9, no. 4, pp. 835–843, Aug. 2024, doi: https://doi.org/10.33889/ijmems.2024.9.4.043